NLO Photon PDF

parametrization using ee and ep data

H. Abramowicz, A. Levy, W. Slominski

A global fit to:

- e^+e^- : $\gamma + \gamma* \rightarrow$ hadrons *done*
- Di-jets PHP at HERA: $\gamma + p \rightarrow$ hadrons *done*
- Di-jets PHP at LEP: $\gamma + \gamma* \rightarrow$ hadrons *plan for future*
- Heavy flavour PHP: $\gamma + p \rightarrow c/b$ hadrons *plan for future*

Comparison with other NLO parametrizations

Q_0^2 of the input PDFs $f_j^\gamma(x, Q_0^2)$
GRV: $0.25\,\mathrm{GeV}^2$,
AFG: $0.5\,\mathrm{GeV}^2$,
ALS: $2.5\,\mathrm{GeV}^2$.

We use proton input at low x for $Q^2 \geq 2.7\,\mathrm{GeV}^2$.

We take $m_c = 1.5\,\mathrm{GeV}$ and thus our $Q_0^2 = 2.5\,\mathrm{GeV}^2$ is just above the charm threshold. Thus we have initial charm quark distribution.

We go "backwards" (to lower Q^2) in our NLO evolution. There is a risk of getting unphysical results (as negative cross sections) — this is a signal for a bad initial parametrization. In practice we go down to $1.8\,\mathrm{GeV}^2$ only.

Our input parametrization has free parameters in both point-like and hadronic parts. The other two parametrizations have (at their low Q_0^2) a VDM-like (hadronic) input only.

Comment on photon vs. proton PDFs

- Proton evolution eqs are homogenous and at any Q^2 PDFs are 'proportional' to the input ones.

- In the photon case evolution eqs are inhomogenous. With growing Q^2, the sensitivity to the input parametrization moves to lower and lower x, and at finite x photon PDFs are radiatively generated by QCD. Hence, in this region, we hardly test the input parametrization — we rather test QCD (who wants this any more?..) and heavy quarks behaviour around thresholds.

Parametrization

$$f_q(x) = f_{\bar{q}}(x) = e_q^2 A^{\mathsf{PL}} \frac{x^2 + (1-x)^2}{1 - B^{\mathsf{PL}} \ln(1-x)} + f_q^{\mathsf{HAD}}(x)$$

$$f_u^{\mathsf{HAD}}(x) = f_d^{\mathsf{HAD}}(x) = A^{\mathsf{HAD}} x^{B^{\mathsf{HAD}}} (1-x)^{C^{\mathsf{HAD}}} \left(1 + D^{\mathsf{HAD}} x\right)$$

$$f_s^{\mathsf{HAD}}(x) = 0.3 f_d^{\mathsf{HAD}}(x)$$

$$f_c^{\mathsf{HAD}}(x) = A_c^{\mathsf{HAD}} x^{B_c^{\mathsf{HAD}}} (1-x)^{C_c^{\mathsf{HAD}}}$$

$$f_G(x) = A_G^{\mathsf{HAD}} x^{B_G^{\mathsf{HAD}}} (1-x)^{C_G^{\mathsf{HAD}}}$$

12 parameters.

DISγ scheme

$$\mathcal{F}_2 = \sum_q 2e_q^2 f_q^\gamma + \frac{\alpha_s}{2\pi} C_{F,2}^{(1)} \otimes \sum_q 2e_q^2 f_{q0}^\gamma + \langle e^2 \rangle C_{G,2} \otimes f_{G0}^\gamma$$

Terms in red are NLO and f_{q0}^γ are evolved at LO.

For heavy quarks we replace $f_h^\gamma \to (1 - \mathcal{S}) f_h^\gamma$ and add a Bethe-Heitler contribution, $\mathcal{S}\mathcal{F}_2^{\mathrm{B-H}}$ to $\mathcal{F}_2$. In the following the suppression factor $\mathcal{S}$ is defined as

$$\mathcal{S} = \frac{\log \frac{m_h^2}{\mu_0^2}}{\log \frac{W^2}{4\mu_0^2}}$$

with $\mu_0^2 = 1.2\,\Lambda_3^2$.

We have also done fits with $\mathcal{S} = 0$ and $\mathcal{S} = 1$. The fits have similar χ^2 and result in not very much different PDFs.

We need exclusive heavy flavour processes.

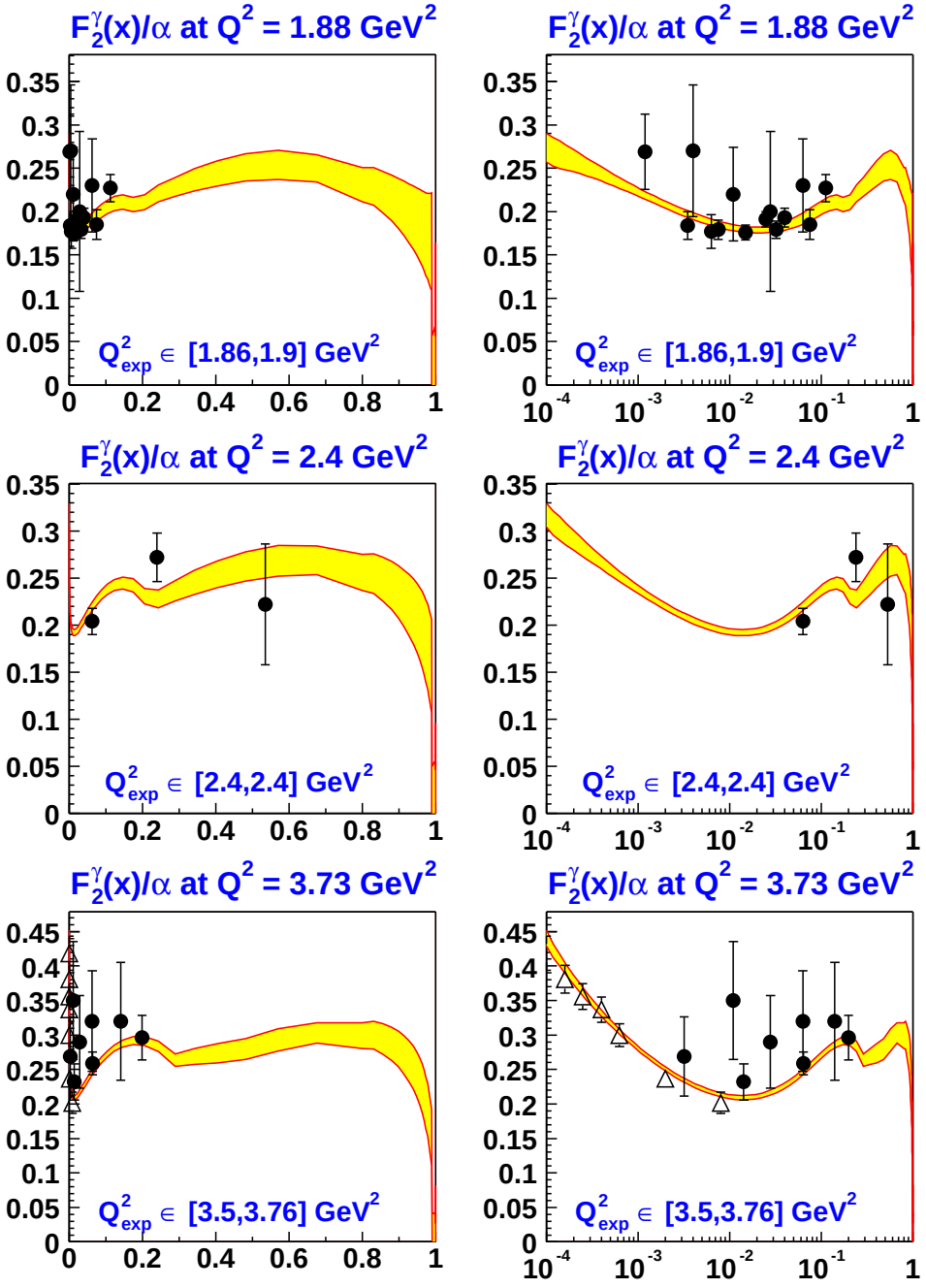

Results of the fit

We use the following data points:

177 F_2^γ from ee

114 F_2^p from ep

24 $\frac{d\sigma}{dE_\perp\, dx_\gamma^{\rm obs}}$ from PHP dijets

Fit to 291 F_2 points gives

$\chi^2 = 260$, $\chi^2/\text{NDF} = 0.9$

Fit to 315 F_2 + dijets points gives

$\chi^2 = 401$, $\chi^2/\text{NDF} = 1.3$

$\chi^2_{\rm dijets} = 141$!!!

The curves in the plots are drawn at Q^2 given above the graph. The data points are within the $Q^2_{\rm exp}$ range.

Full dots — F_2^γ data

Triangles — F_2^p data

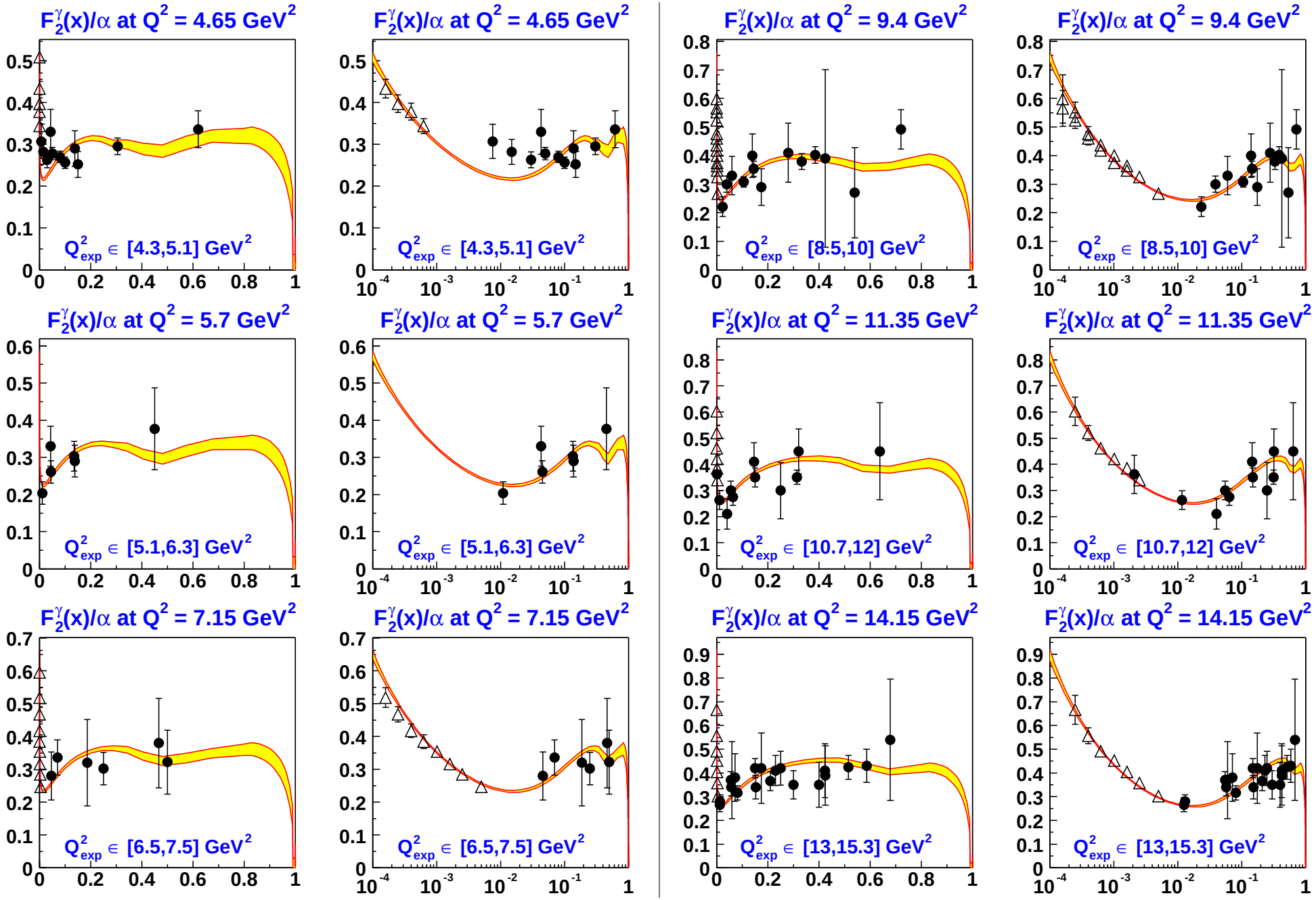
$F_2^\gamma(x)/\alpha$ at Q^2 = 4.65 GeV^2
$Q^2_{exp} \in$ [4.3,5.1] GeV^2
$F_2^\gamma(x)/\alpha$ at Q^2 = 4.65 GeV^2
$Q^2_{exp} \in$ [4.3,5.1] GeV^2
$F_2^\gamma(x)/\alpha$ at Q^2 = 9.4 GeV^2
$Q^2_{exp} \in$ [8.5,10] GeV^2
$F_2^\gamma(x)/\alpha$ at Q^2 = 9.4 GeV^2
$Q^2_{exp} \in$ [8.5,10] GeV^2
$F_2^\gamma(x)/\alpha$ at Q^2 = 5.7 GeV^2
$Q^2_{exp} \in$ [5.1,6.3] GeV^2
$F_2^\gamma(x)/\alpha$ at Q^2 = 5.7 GeV^2
$Q^2_{exp} \in$ [5.1,6.3] GeV^2
$F_2^\gamma(x)/\alpha$ at Q^2 = 11.35 GeV^2
$Q^2_{exp} \in$ [10.7,12] GeV^2
$F_2^\gamma(x)/\alpha$ at Q^2 = 11.35 GeV^2
$Q^2_{exp} \in$ [10.7,12] GeV^2
$F_2^\gamma(x)/\alpha$ at Q^2 = 7.15 GeV^2
$Q^2_{exp} \in$ [6.5,7.5] GeV^2
$F_2^\gamma(x)/\alpha$ at Q^2 = 7.15 GeV^2
$Q^2_{exp} \in$ [6.5,7.5] GeV^2
$F_2^\gamma(x)/\alpha$ at Q^2 = 14.15 GeV^2
$Q^2_{exp} \in$ [13,15.3] GeV^2
$F_2^\gamma(x)/\alpha$ at Q^2 = 14.15 GeV^2
$Q^2_{exp} \in$ [13,15.3] GeV^2

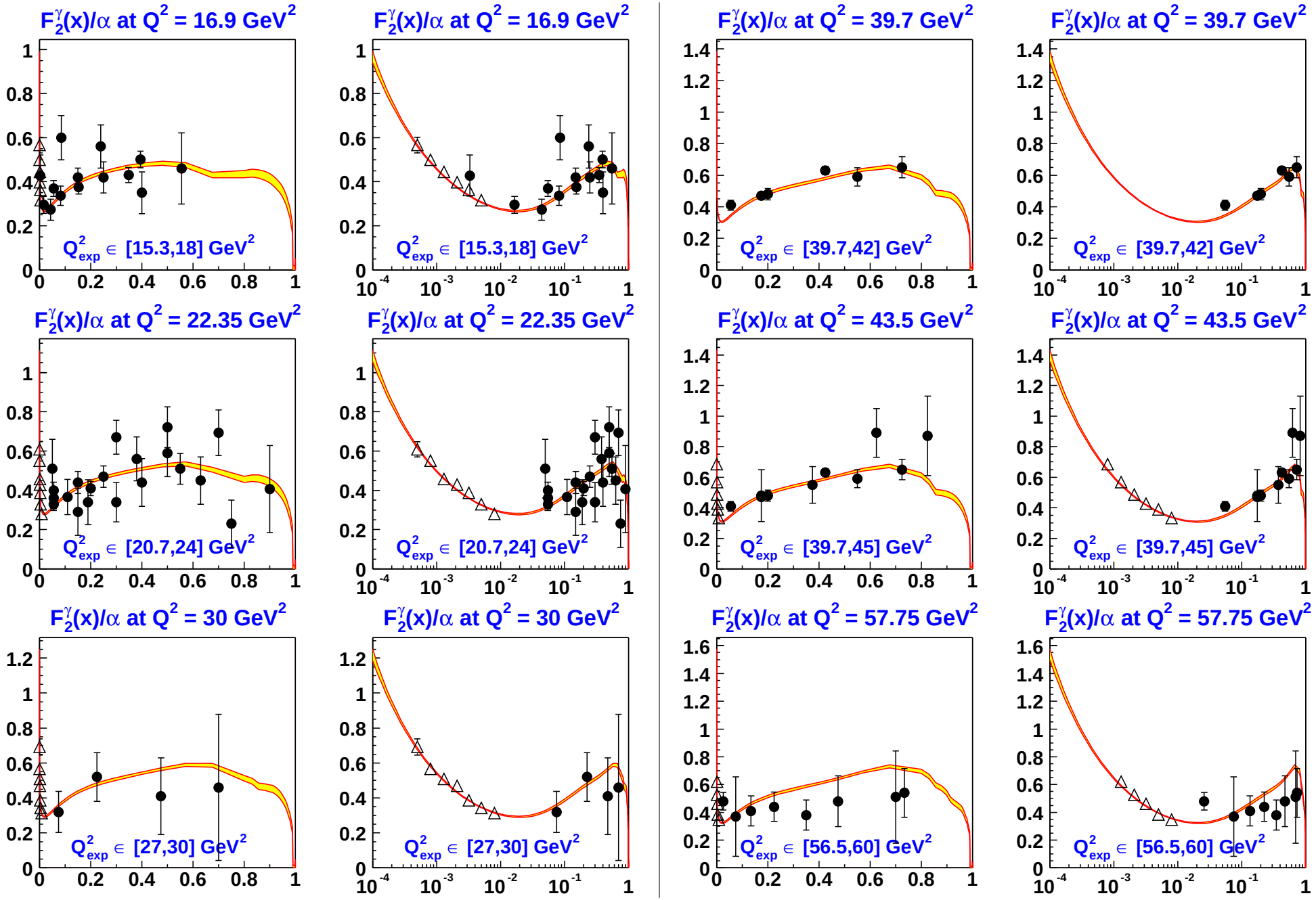
$F_2^\gamma(x)/\alpha$ at Q^2 = 16.9 GeV^2
$Q^2_{exp} \in$ [15.3,18] GeV^2
$F_2^\gamma(x)/\alpha$ at Q^2 = 16.9 GeV^2
$Q^2_{exp} \in$ [15.3,18] GeV^2
$F_2^\gamma(x)/\alpha$ at Q^2 = 39.7 GeV^2
$Q^2_{exp} \in$ [39.7,42] GeV^2
$F_2^\gamma(x)/\alpha$ at Q^2 = 39.7 GeV^2
$Q^2_{exp} \in$ [39.7,42] GeV^2
$F_2^\gamma(x)/\alpha$ at Q^2 = 22.35 GeV^2
$Q^2_{exp} \in$ [20.7,24] GeV^2
$F_2^\gamma(x)/\alpha$ at Q^2 = 22.35 GeV^2
$Q^2_{exp} \in$ [20.7,24] GeV^2
$F_2^\gamma(x)/\alpha$ at Q^2 = 43.5 GeV^2
$Q^2_{exp} \in$ [39.7,45] GeV^2
$F_2^\gamma(x)/\alpha$ at Q^2 = 43.5 GeV^2
$Q^2_{exp} \in$ [39.7,45] GeV^2
$F_2^\gamma(x)/\alpha$ at Q^2 = 30 GeV^2
$Q^2_{exp} \in$ [27,30] GeV^2
$F_2^\gamma(x)/\alpha$ at Q^2 = 30 GeV^2
$Q^2_{exp} \in$ [27,30] GeV^2
$F_2^\gamma(x)/\alpha$ at Q^2 = 57.75 GeV^2
$Q^2_{exp} \in$ [56.5,60] GeV^2
$F_2^\gamma(x)/\alpha$ at Q^2 = 57.75 GeV^2
$Q^2_{exp} \in$ [56.5,60] GeV^2

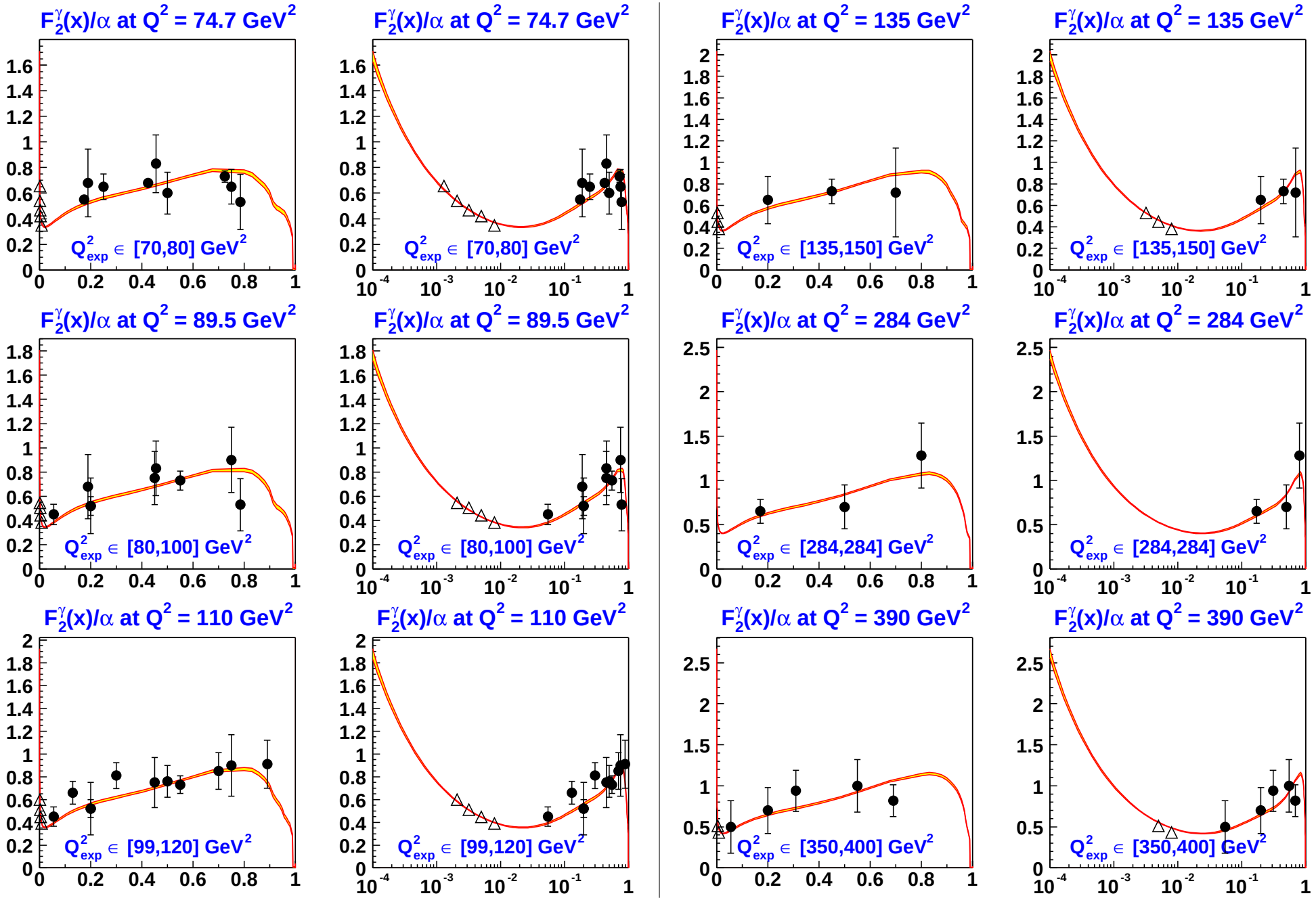
$F_2^\gamma(x)/\alpha$ at Q^2 = 74.7 GeV^2
$Q^2_{exp} \in$ [70,80] GeV^2
$F_2^\gamma(x)/\alpha$ at Q^2 = 74.7 GeV^2
$Q^2_{exp} \in$ [70,80] GeV^2
$F_2^\gamma(x)/\alpha$ at Q^2 = 135 GeV^2
$Q^2_{exp} \in$ [135,150] GeV^2
$F_2^\gamma(x)/\alpha$ at Q^2 = 135 GeV^2
$Q^2_{exp} \in$ [135,150] GeV^2
$F_2^\gamma(x)/\alpha$ at Q^2 = 89.5 GeV^2
$Q^2_{exp} \in$ [80,100] GeV^2
$F_2^\gamma(x)/\alpha$ at Q^2 = 89.5 GeV^2
$Q^2_{exp} \in$ [80,100] GeV^2
$F_2^\gamma(x)/\alpha$ at Q^2 = 284 GeV^2
$Q^2_{exp} \in$ [284,284] GeV^2
$F_2^\gamma(x)/\alpha$ at Q^2 = 284 GeV^2
$Q^2_{exp} \in$ [284,284] GeV^2
$F_2^\gamma(x)/\alpha$ at Q^2 = 110 GeV^2
$Q^2_{exp} \in$ [99,120] GeV^2
$F_2^\gamma(x)/\alpha$ at Q^2 = 110 GeV^2
$Q^2_{exp} \in$ [99,120] GeV^2
$F_2^\gamma(x)/\alpha$ at Q^2 = 390 GeV^2
$Q^2_{exp} \in$ [350,400] GeV^2
$F_2^\gamma(x)/\alpha$ at Q^2 = 390 GeV^2
$Q^2_{exp} \in$ [350,400] GeV^2

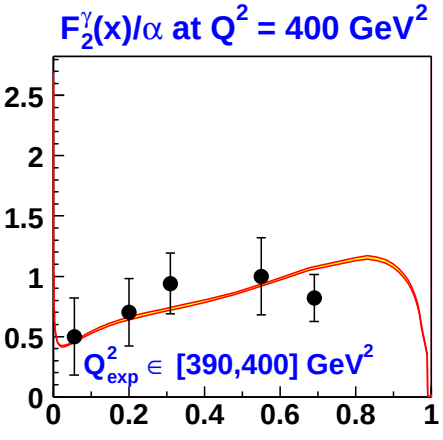
$F_2^\gamma(x)/\alpha$ at Q^2 = 400 GeV^2
$Q^2_{exp} \in$ [390,400] GeV^2

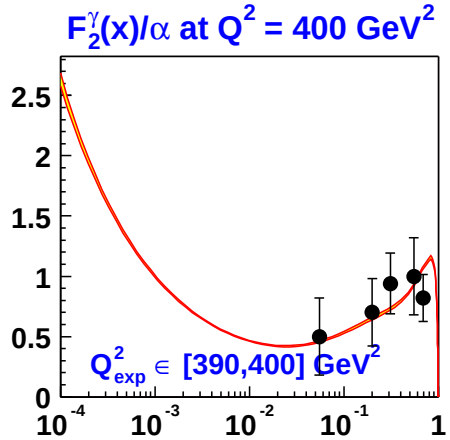
$F_2^\gamma(x)/\alpha$ at Q^2 = 400 GeV^2
$Q^2_{exp} \in$ [390,400] GeV^2

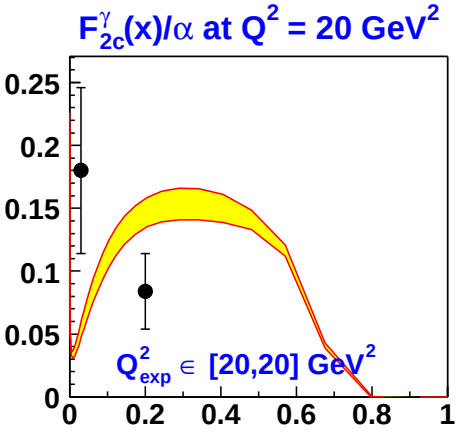
$F_{2c}^\gamma(x)/\alpha$ at Q^2 = 20 GeV^2
$Q^2_{exp} \in$ [20,20] GeV^2

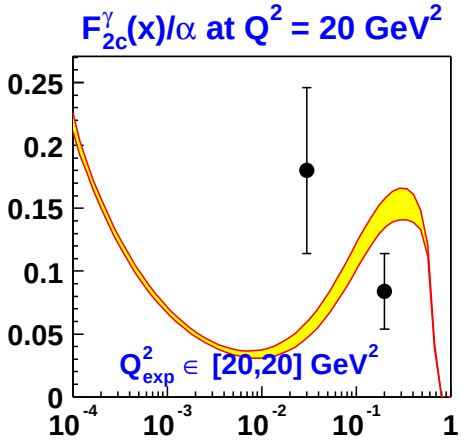
$F_{2c}^\gamma(x)/\alpha$ at Q^2 = 20 GeV^2
$Q^2_{exp} \in$ [20,20] GeV^2

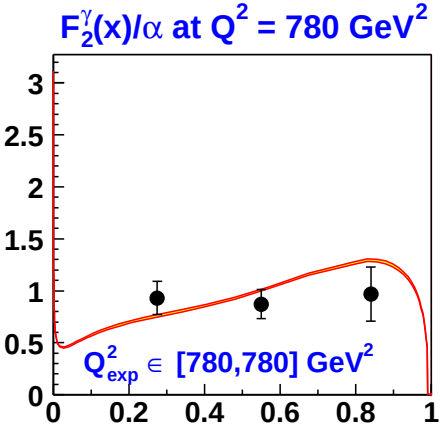
$F_2^\gamma(x)/\alpha$ at Q^2 = 780 GeV^2
$Q^2_{exp} \in$ [780,780] GeV^2

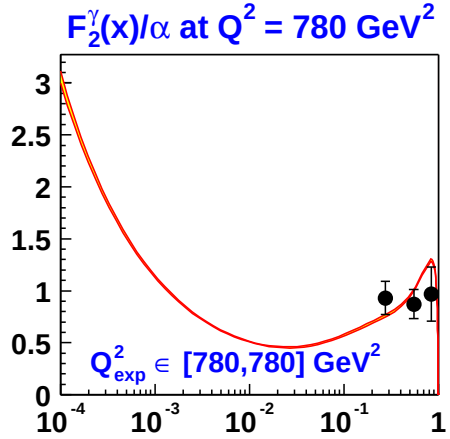
$F_2^\gamma(x)/\alpha$ at Q^2 = 780 GeV^2
$Q^2_{exp} \in$ [780,780] GeV^2

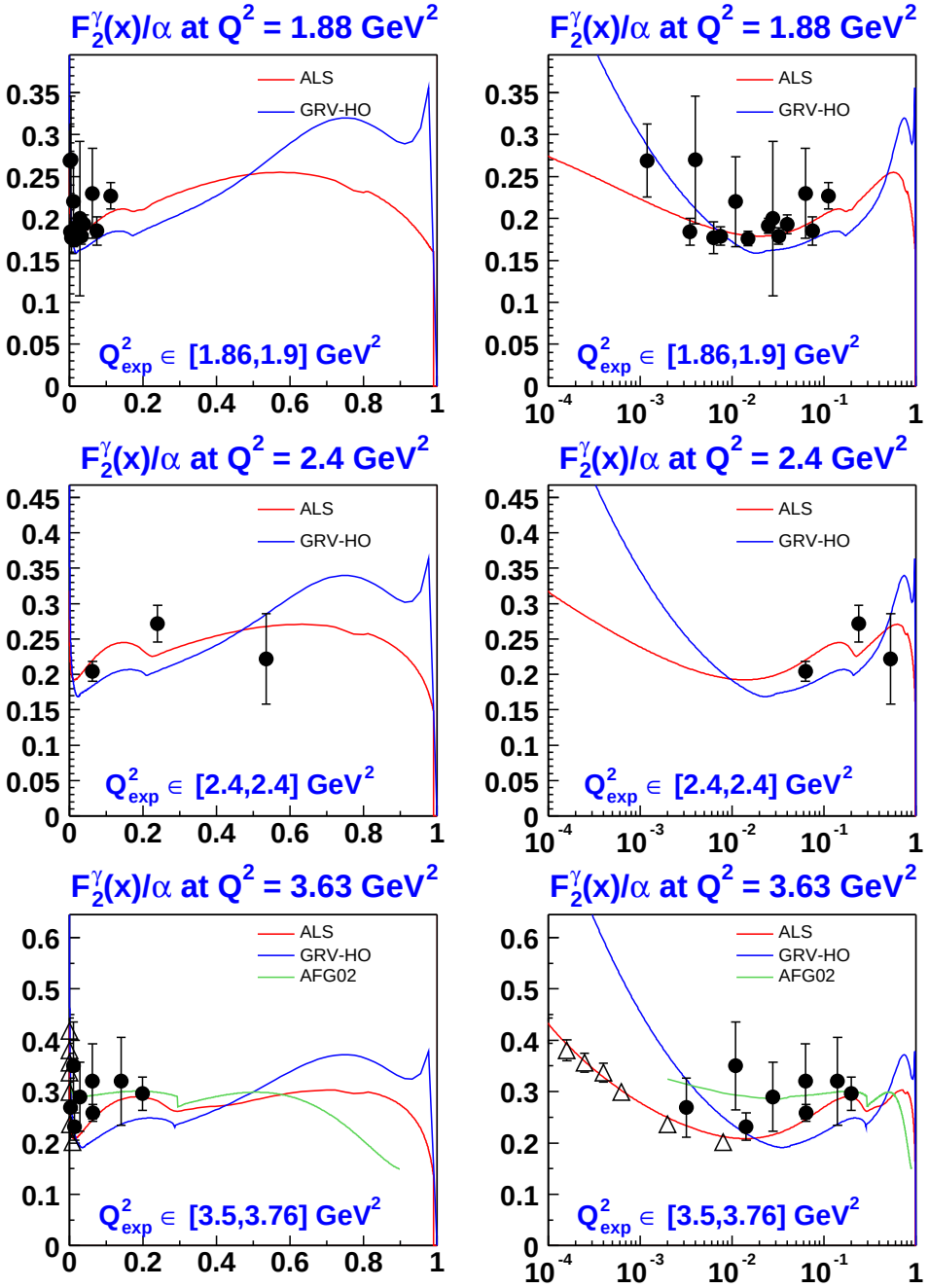

ALS vs. GRV & AFG

Comparison of F_2^γ NLO parametrizations with available e^+e^- and ep data.

ALS

GRV-HO

AFG v. 02

$x \in [0.002, 0.9], Q^2 > 2.5\text{GeV}^2$

Full dots — F_2^γ data

Triangles — F_2^p data

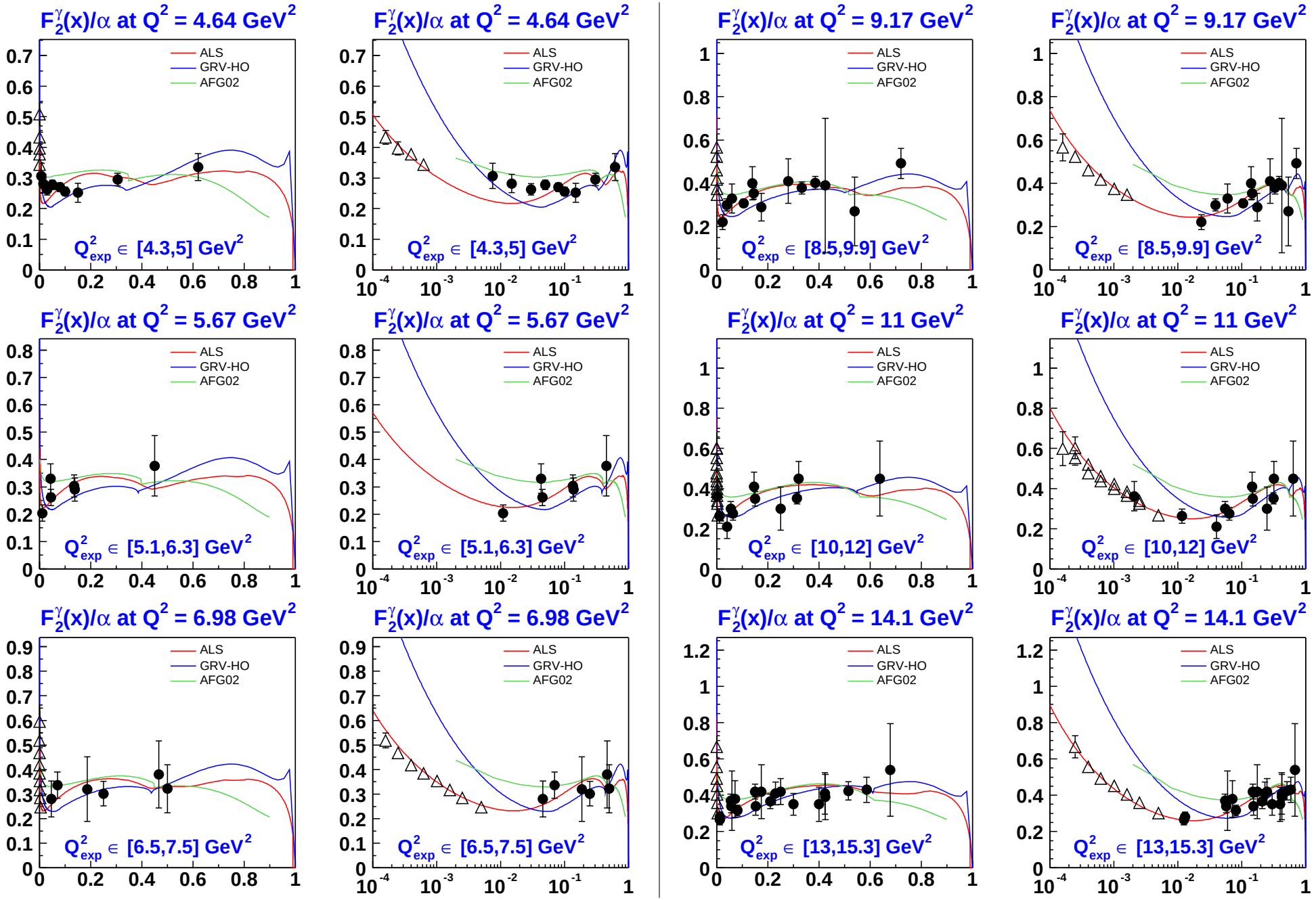
$F_2^\gamma(x)/\alpha$ at Q^2 = 4.64 GeV^2
$Q^2_{exp} \in$ [4.3,5] GeV^2
$F_2^\gamma(x)/\alpha$ at Q^2 = 9.17 GeV^2
$Q^2_{exp} \in$ [8.5,9.9] GeV^2
$F_2^\gamma(x)/\alpha$ at Q^2 = 5.67 GeV^2
$Q^2_{exp} \in$ [5.1,6.3] GeV^2
$F_2^\gamma(x)/\alpha$ at Q^2 = 11 GeV^2
$Q^2_{exp} \in$ [10,12] GeV^2
$F_2^\gamma(x)/\alpha$ at Q^2 = 6.98 GeV^2
$Q^2_{exp} \in$ [6.5,7.5] GeV^2
$F_2^\gamma(x)/\alpha$ at Q^2 = 14.1 GeV^2
$Q^2_{exp} \in$ [13,15.3] GeV^2
ALS
GRV-HO
AFG02

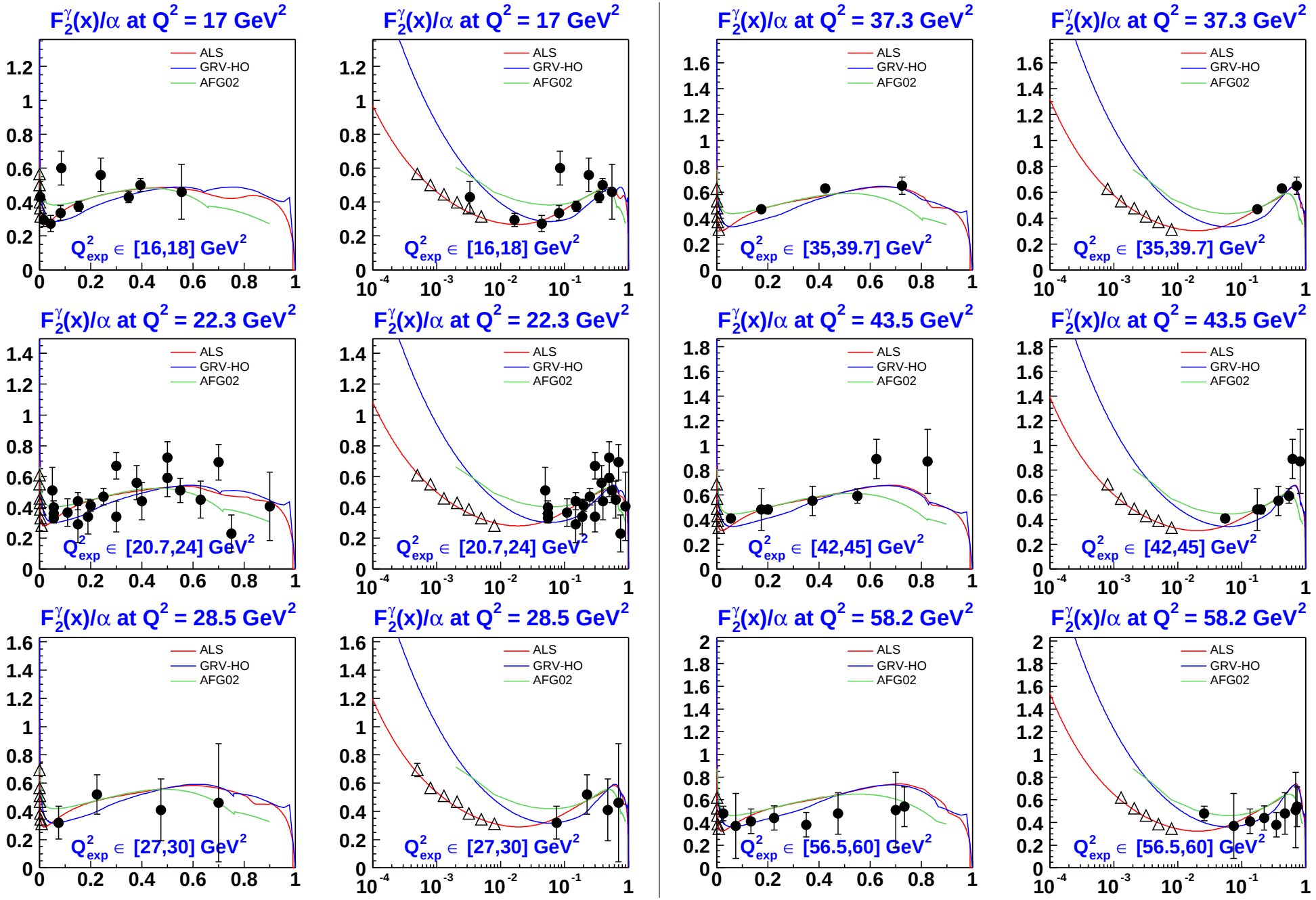
$F_2^\gamma(x)/\alpha$ at Q^2 = 17 GeV^2
$Q^2_{exp} \in$ [16,18] GeV^2
$F_2^\gamma(x)/\alpha$ at Q^2 = 37.3 GeV^2
$Q^2_{exp} \in$ [35,39.7] GeV^2
$F_2^\gamma(x)/\alpha$ at Q^2 = 22.3 GeV^2
$Q^2_{exp} \in$ [20.7,24] GeV^2
$F_2^\gamma(x)/\alpha$ at Q^2 = 43.5 GeV^2
$Q^2_{exp} \in$ [42,45] GeV^2
$F_2^\gamma(x)/\alpha$ at Q^2 = 28.5 GeV^2
$Q^2_{exp} \in$ [27,30] GeV^2
$F_2^\gamma(x)/\alpha$ at Q^2 = 58.2 GeV^2
$Q^2_{exp} \in$ [56.5,60] GeV^2
ALS
GRV-HO
AFG02

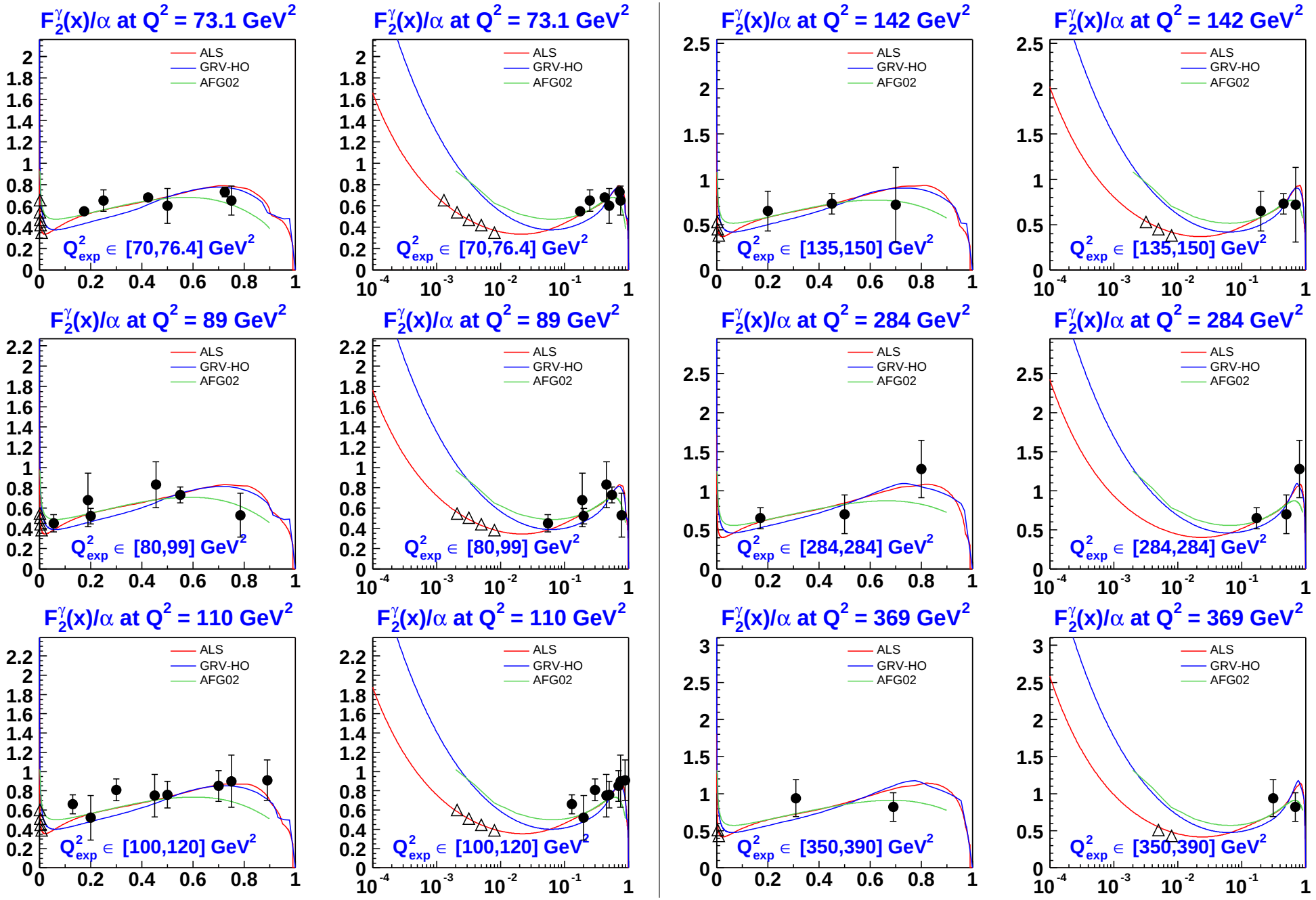
$F_2^\gamma(x)/\alpha$ at Q^2 = 73.1 GeV^2
$Q^2_{exp} \in$ [70,76.4] GeV^2
$F_2^\gamma(x)/\alpha$ at Q^2 = 142 GeV^2
$Q^2_{exp} \in$ [135,150] GeV^2
$F_2^\gamma(x)/\alpha$ at Q^2 = 89 GeV^2
$Q^2_{exp} \in$ [80,99] GeV^2
$F_2^\gamma(x)/\alpha$ at Q^2 = 284 GeV^2
$Q^2_{exp} \in$ [284,284] GeV^2
$F_2^\gamma(x)/\alpha$ at Q^2 = 110 GeV^2
$Q^2_{exp} \in$ [100,120] GeV^2
$F_2^\gamma(x)/\alpha$ at Q^2 = 369 GeV^2
$Q^2_{exp} \in$ [350,390] GeV^2
ALS
GRV-HO
AFG02

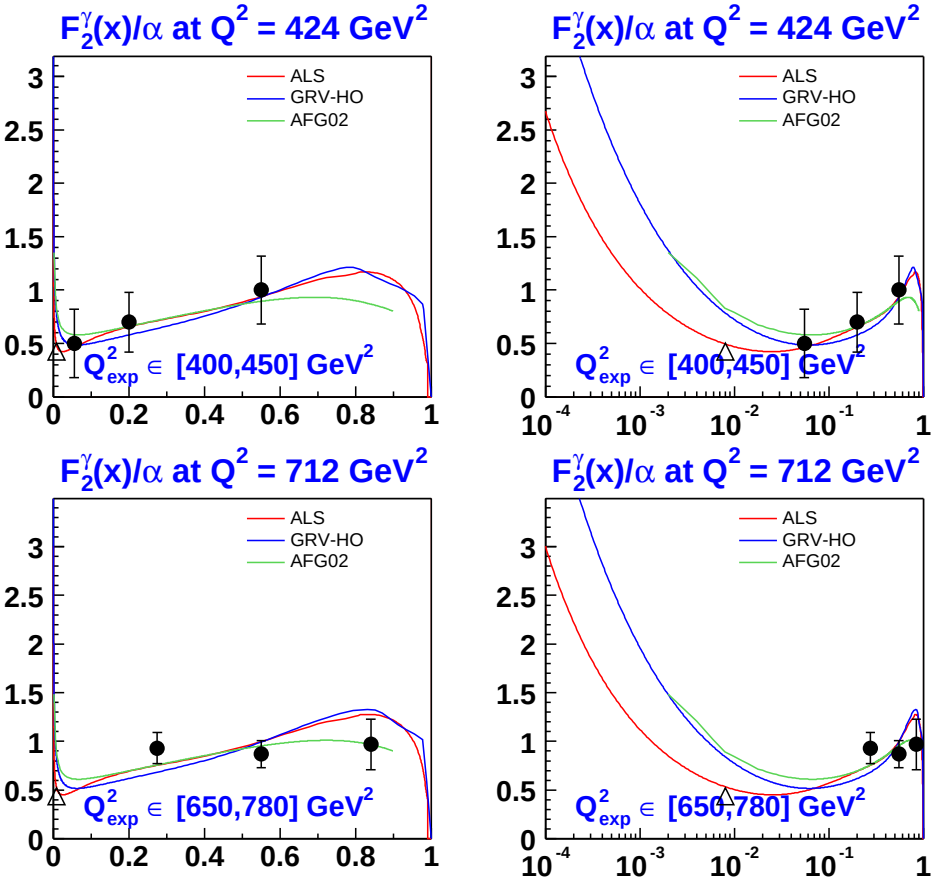
$F_2^\gamma(x)/\alpha$ at Q^2 = 424 GeV^2
ALS
GRV-HO
AFG02
$Q^2_{exp} \in$ [400,450] GeV^2
$F_2^\gamma(x)/\alpha$ at Q^2 = 424 GeV^2
ALS
GRV-HO
AFG02
$Q^2_{exp} \in$ [400,450] GeV^2
$F_2^\gamma(x)/\alpha$ at Q^2 = 712 GeV^2
ALS
GRV-HO
AFG02
$Q^2_{exp} \in$ [650,780] GeV^2
$F_2^\gamma(x)/\alpha$ at Q^2 = 712 GeV^2
ALS
GRV-HO
AFG02
$Q^2_{exp} \in$ [650,780] GeV^2

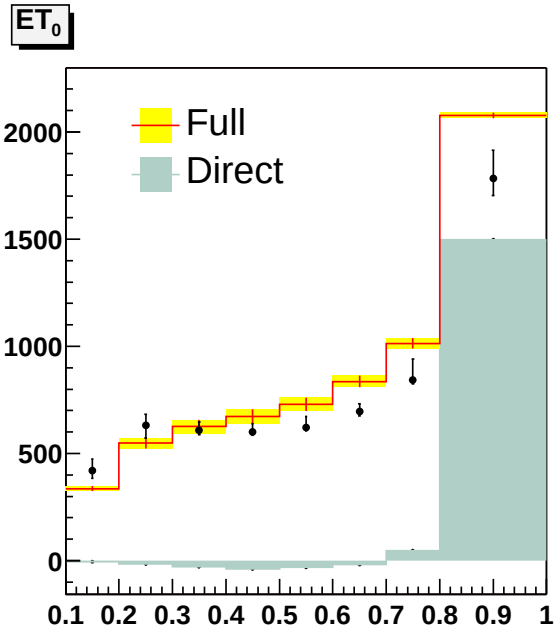

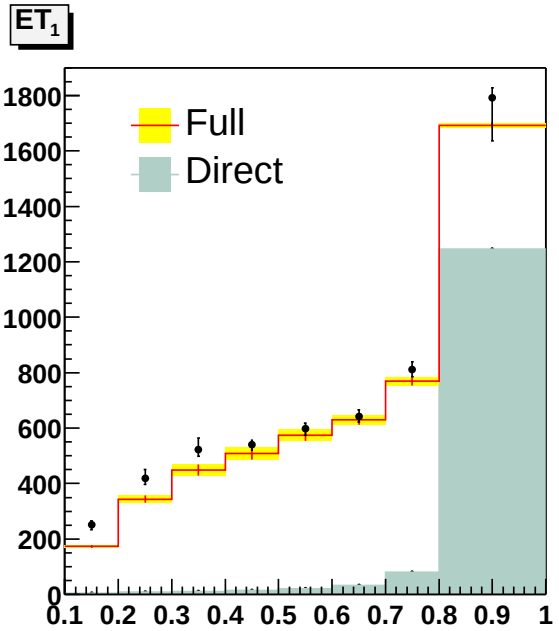

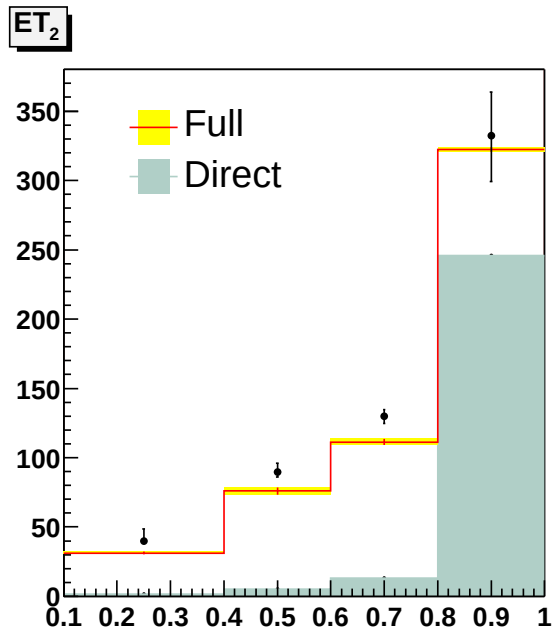

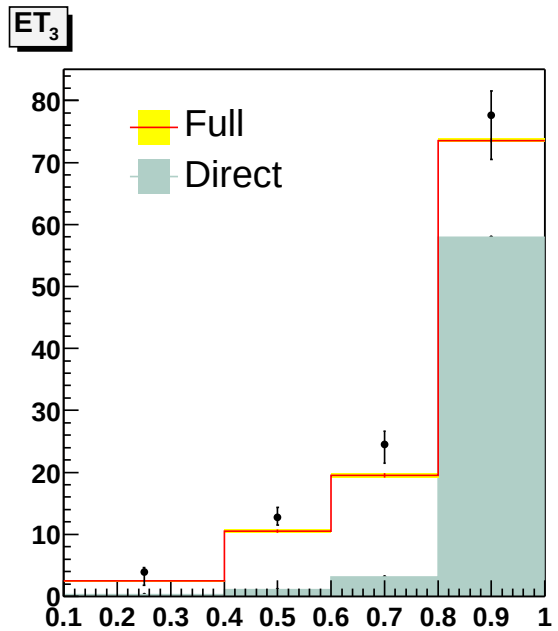

Di-jets PHP

$$\frac{d\sigma}{dx_\gamma^{\rm obs}}[pb]$$

in 4 $E_\perp$(GeV) bins:
14 – 17, 17 – 25,
25 – 35, 35 – 90.

24 dijet PHP points measured by ZEUS

Eur. Phys. J. C23 (2002) 615

$\chi^2_{\rm dijets} = 141$

The yellow bands mark the fit uncertainty.

The histograms are calculated using the Frixione code with ALS parametrization added.

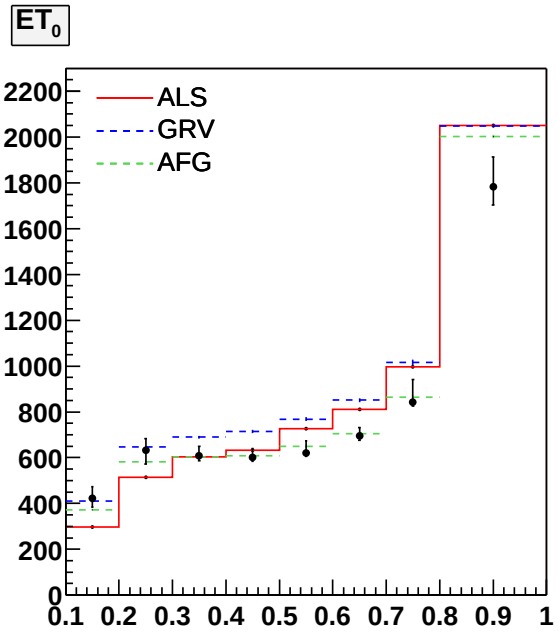

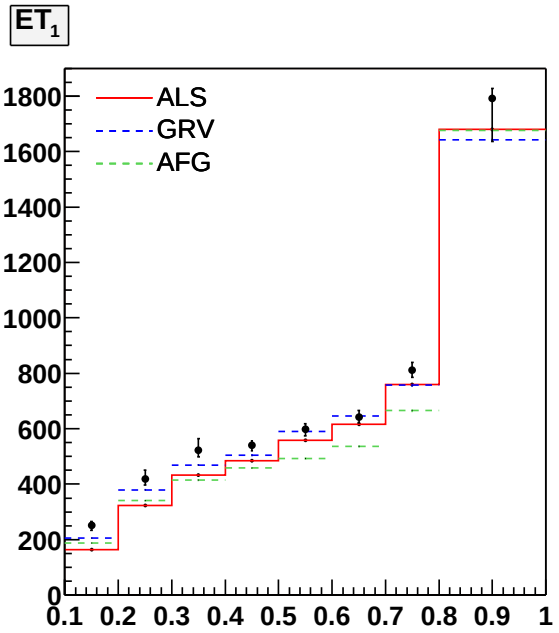

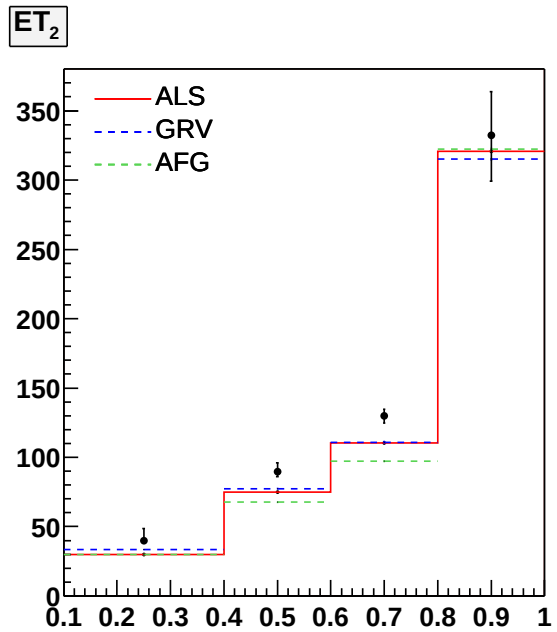

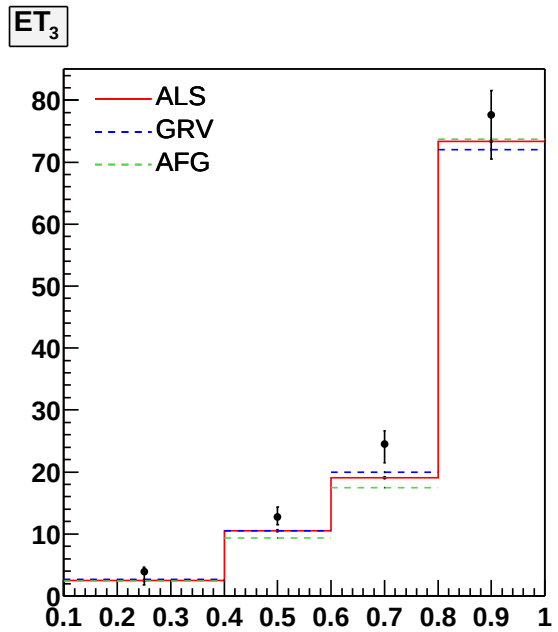

Comparison of ALS, GRV and AFG

$$\frac{d\sigma}{dx_\gamma^{\rm obs}}[pb]$$

in 4 $E_\perp$(GeV) bins:
14 – 17, 17 – 25,
25 – 35, 35 – 90.

Dijet PHP points measured by ZEUS

Eur. Phys. J. C23 (2002) 615

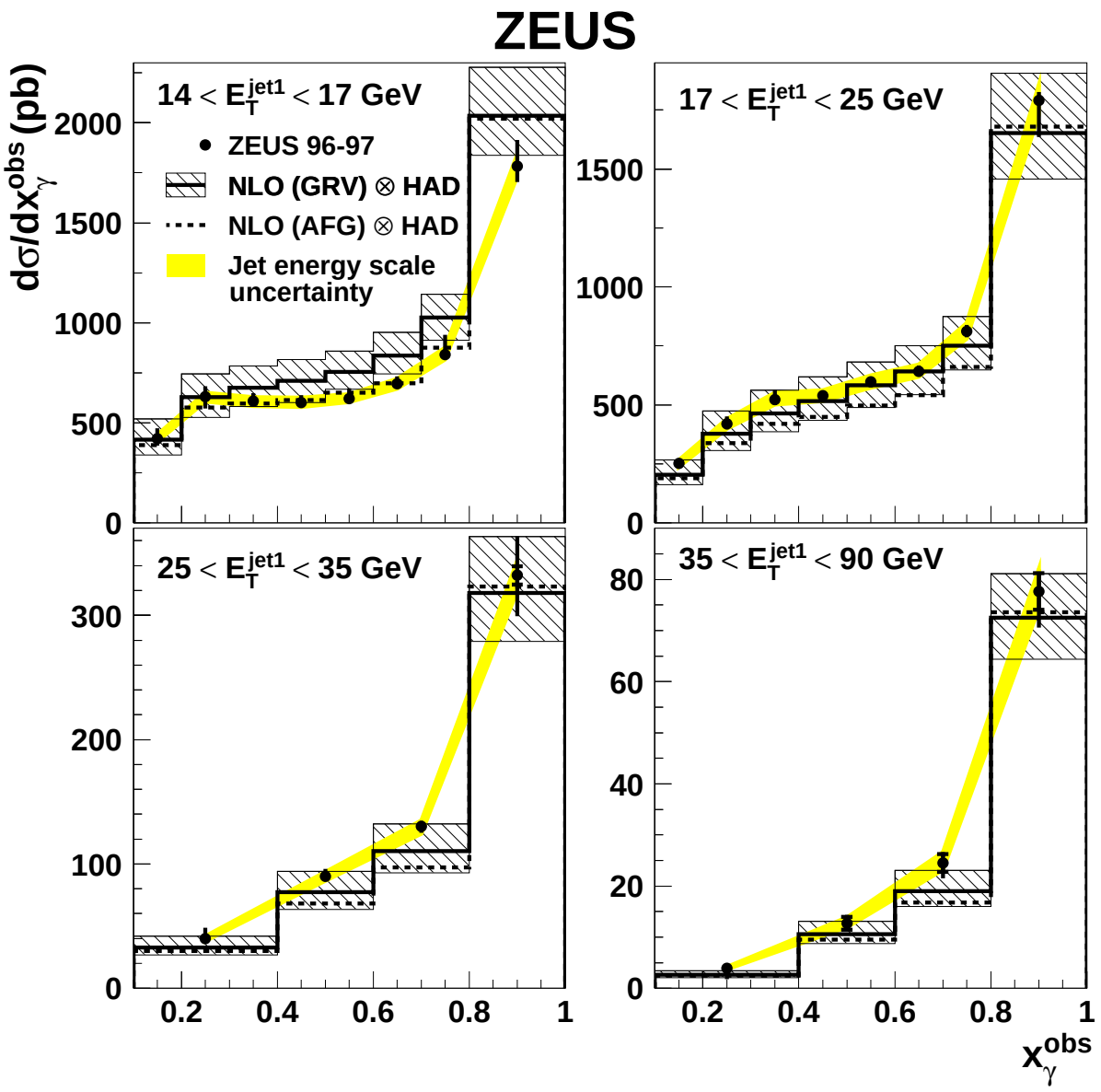
ZEUS
$14 < E_T^{jet1} < 17$ GeV
$17 < E_T^{jet1} < 25$ GeV
$25 < E_T^{jet1} < 35$ GeV
$35 < E_T^{jet1} < 90$ GeV
ZEUS 96-97
NLO (GRV) ⊗ HAD
NLO (AFG) ⊗ HAD
Jet energy scale uncertainty
$d\sigma/dx_\gamma^{obs}$ (pb)
x_γ^{obs}

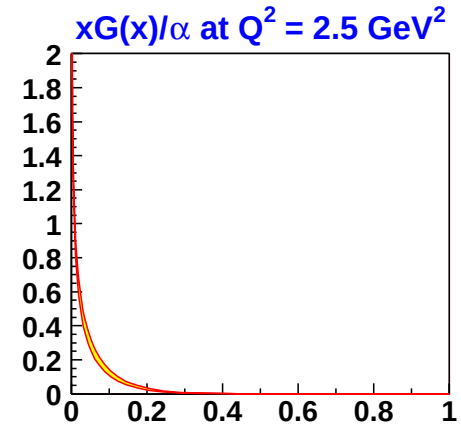
xG(x)/α at Q² = 2.5 GeV²

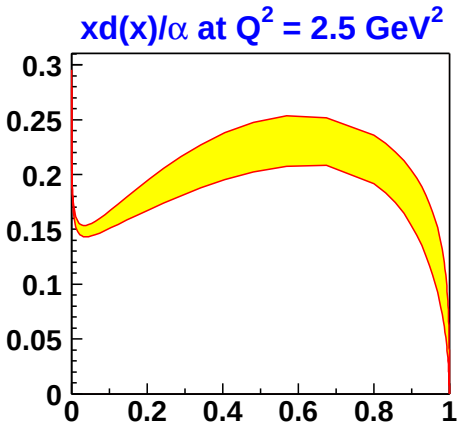
xd(x)/α at Q² = 2.5 GeV²

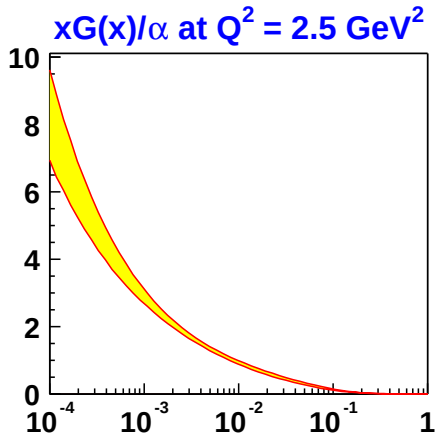
xG(x)/α at Q² = 2.5 GeV²

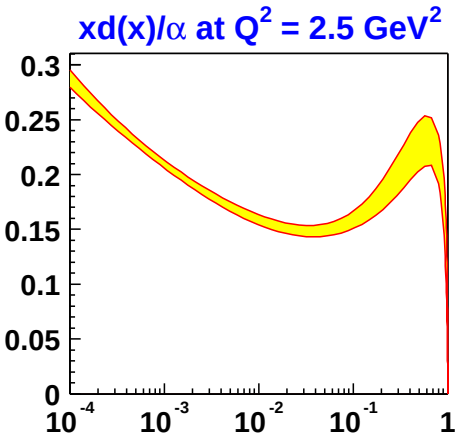
xd(x)/α at Q² = 2.5 GeV²

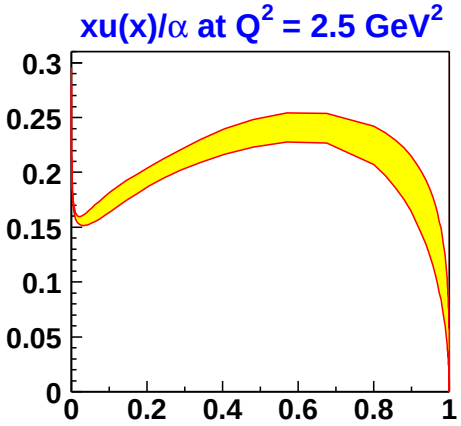
xu(x)/α at Q² = 2.5 GeV²

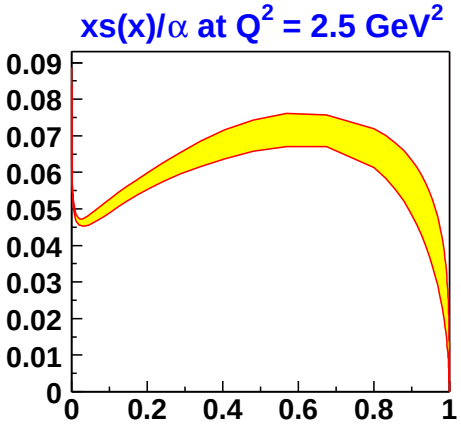
xs(x)/α at Q² = 2.5 GeV²

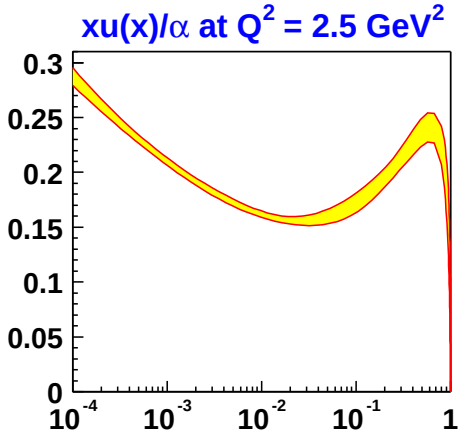
xu(x)/α at Q² = 2.5 GeV²

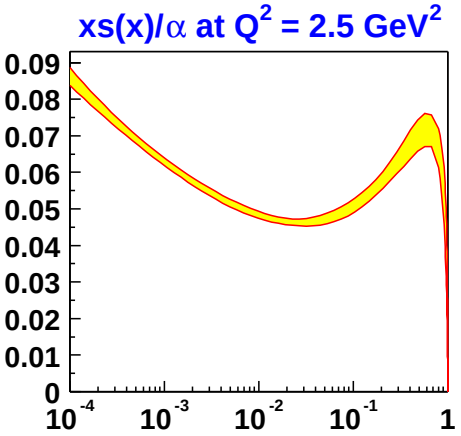
xs(x)/α at Q² = 2.5 GeV²

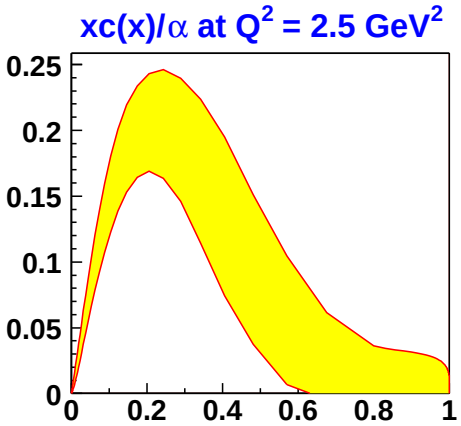
xc(x)/α at Q² = 2.5 GeV²

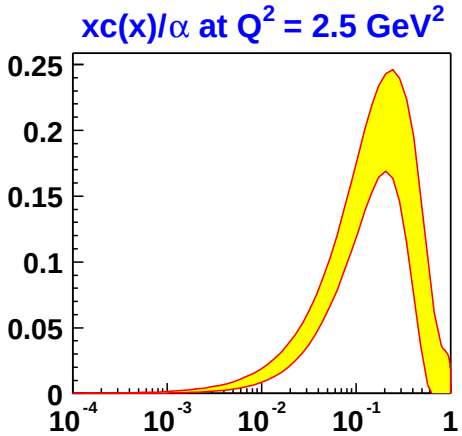
xc(x)/α at Q² = 2.5 GeV²

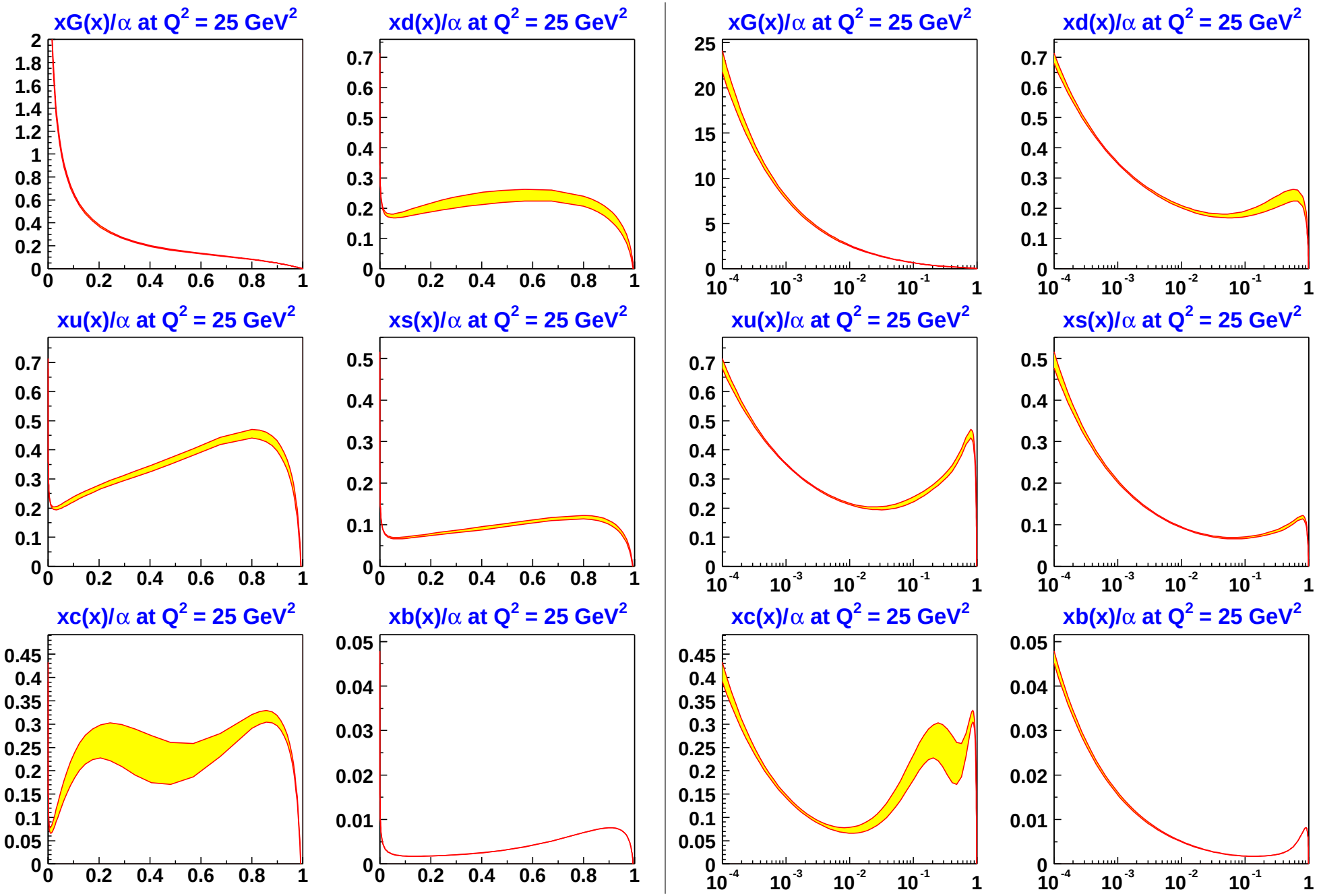
xG(x)/α at Q² = 25 GeV²
xd(x)/α at Q² = 25 GeV²
xG(x)/α at Q² = 25 GeV²
xd(x)/α at Q² = 25 GeV²
xu(x)/α at Q² = 25 GeV²
xs(x)/α at Q² = 25 GeV²
xu(x)/α at Q² = 25 GeV²
xs(x)/α at Q² = 25 GeV²
xc(x)/α at Q² = 25 GeV²
xb(x)/α at Q² = 25 GeV²
xc(x)/α at Q² = 25 GeV²
xb(x)/α at Q² = 25 GeV²

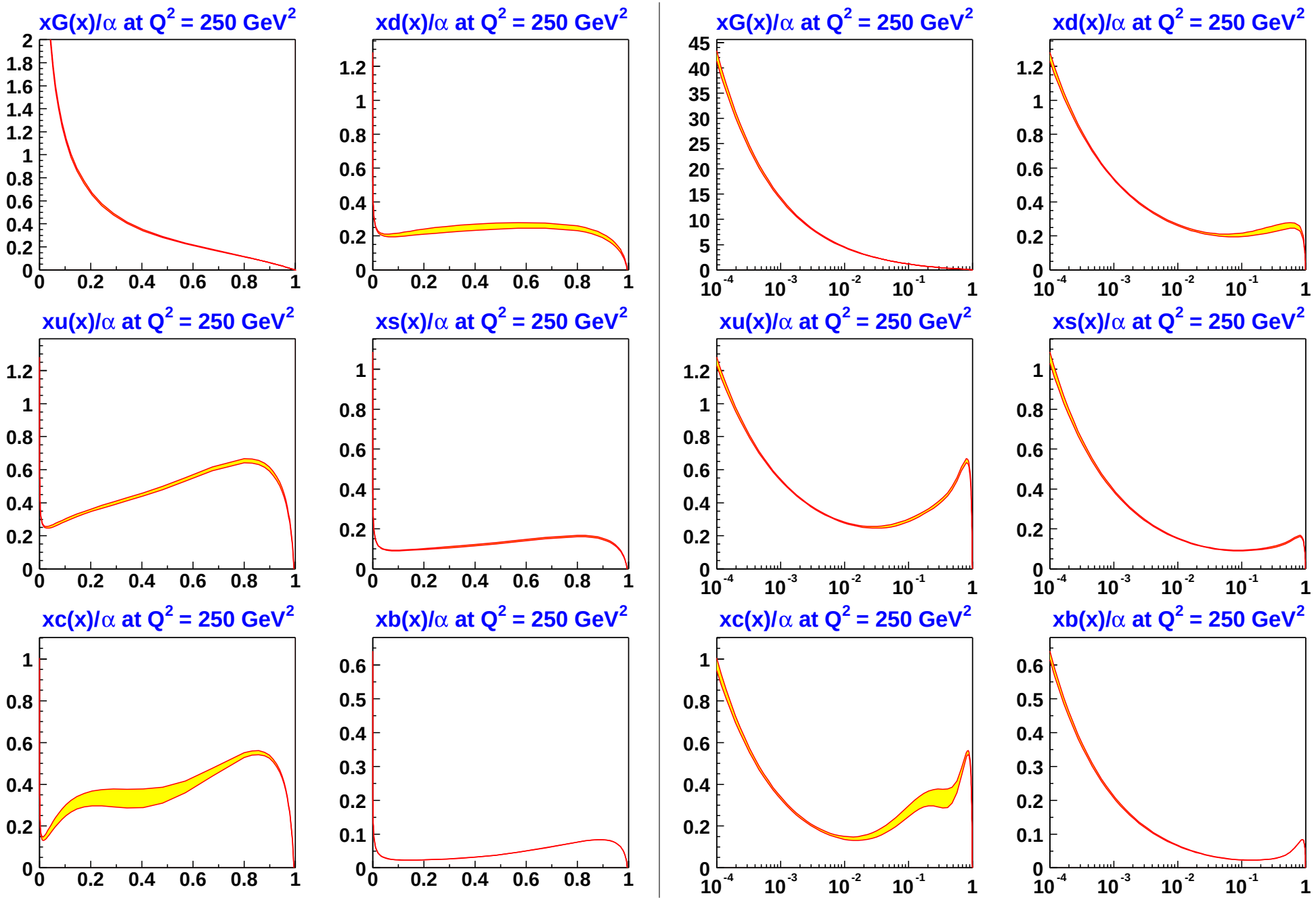
xG(x)/α at Q² = 250 GeV²
xd(x)/α at Q² = 250 GeV²
xG(x)/α at Q² = 250 GeV²
xd(x)/α at Q² = 250 GeV²
xu(x)/α at Q² = 250 GeV²
xs(x)/α at Q² = 250 GeV²
xu(x)/α at Q² = 250 GeV²
xs(x)/α at Q² = 250 GeV²
xc(x)/α at Q² = 250 GeV²
xb(x)/α at Q² = 250 GeV²
xc(x)/α at Q² = 250 GeV²
xb(x)/α at Q² = 250 GeV²

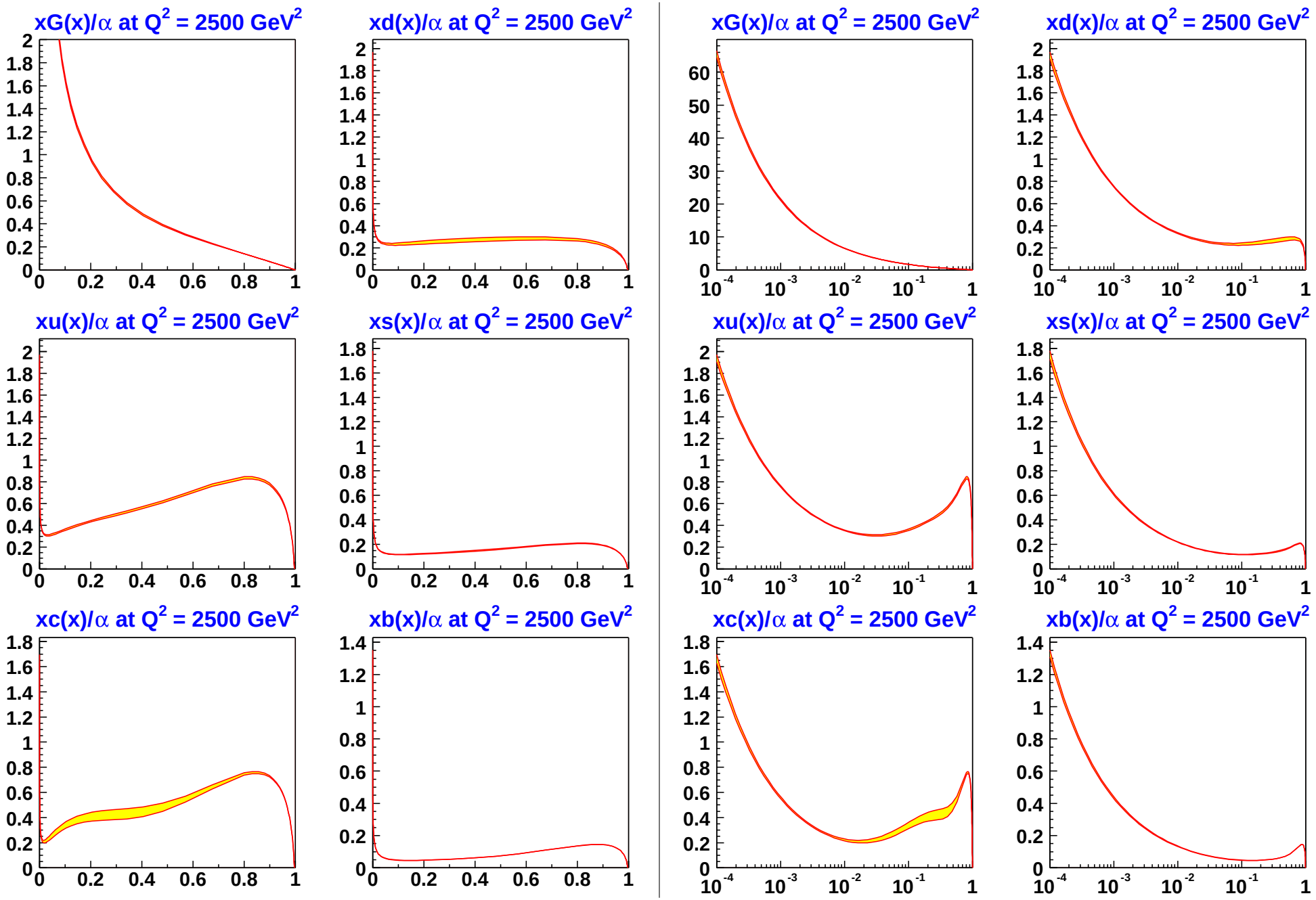
xG(x)/α at Q² = 2500 GeV²
xd(x)/α at Q² = 2500 GeV²
xG(x)/α at Q² = 2500 GeV²
xd(x)/α at Q² = 2500 GeV²
xu(x)/α at Q² = 2500 GeV²
xs(x)/α at Q² = 2500 GeV²
xu(x)/α at Q² = 2500 GeV²
xs(x)/α at Q² = 2500 GeV²
xc(x)/α at Q² = 2500 GeV²
xb(x)/α at Q² = 2500 GeV²
xc(x)/α at Q² = 2500 GeV²
xb(x)/α at Q² = 2500 GeV²

Summary & Conclusions

- A good NLO parameterization to F_2^γ data ($\chi^2/\mathrm{df} \sim 0.9$)
- Includes low-x F_2^p data, starts at $Q_0^2 = 2.5$ GeV^2, parameterize point-like and hadronic part.
- Try a fit to both F_2^γ and full σ^{res} for di-jets PHP.
  Does not help constrain gluons: data at too high x.
  Some better understanding of di-jet properties needed.
- Do a global fit to F_2^γ, di-jets PHP and heavy flavour PHP.